Functional interactions of ribosomal intersubunit bridges in *Saccharomyces cerevisiae*

Tiina Tamm[1*], Ivan Kisly[1] and Jaanus Remme[1]

[1] Department of Molecular Biology, Institute of Molecular and Cell Biology, University of Tartu, Tartu 51010, Estonia

*Corresponding author: ttamm@ut.ee

Supplementary Table S1

Supplementary Materials and Methods

Supplementary Figures S1-S6

Table S1. Yeast strains used in this study.

Strain	Strain name	Genotype	Source
TYSC309	WT	*MAT**a** ura3-52 leu2Δ1 his3Δ200 trp1Δ36 Δarg4 Δlys1*	Lab collection
TYSC310		*MAT**α** ura3-52 leu2Δ1 his3Δ200 trp1Δ36 Δarg4 Δlys1*	Lab collection
TYSC360	eB12Δ	*MAT**a** ura3-52 leu2Δ1 his3Δ200 trp1Δ36 Δarg4 Δlys1 Δrpl19A::kanMX6 Δrpl19B::kanMX6 [pRS315-rpl19$_{1-146}$]*	Lab collection (Kisly et al. 2016)
TYSC453		*MAT**α** ura3-52 leu2Δ1 his3Δ200 trp1Δ36 Δarg4 Δlys1 Δrpl24A::hphMX6*	This study
TYSC455		*MAT**α** ura3-52 leu2Δ1 his3Δ200 trp1Δ36 Δarg4 Δlys1 Δrpl24B::hphMX6*	(Kisly et al. 2019)
TYSC488	eL24Δ	*MAT**a** ura3-52 leu2Δ1 his3Δ200 trp1Δ36 Δarg4 Δlys1 Δrpl24A::hphMX6 Δrpl24B::hphMX6*	(Kisly et al. 2019)
TYSC517		*MAT**a** ura3-52 leu2Δ1 his3Δ200 trp1Δ36 Δarg4 Δlys1Δrpl41A::natMX6*	This study
TYSC519		*MAT**α** ura3-52 leu2Δ1 his3Δ200 trp1Δ36 Δarg4 Δlys1Δrpl41A::natMX6*	This study
TYSC523		*MAT**α** ura3-52 leu2Δ1 his3Δ200 trp1Δ36 Δarg4 Δlys1Δrpl41B::natMX6*	This study

TYSC532	eL41Δ	*MAT**a** ura3-52 leu2Δ1 his3Δ200 trp1Δ36 Δarg4 Δlys1 Δrpl41A::natMX6 Δrpl41B::natMX6*	This study
TYSC561	eL24Δ eL41Δ	*MAT**a** ura3-52 leu2Δ1 his3Δ200 trp1Δ36 Δarg4 Δlys1 Δrpl24A::hphMX6 Δrpl24B::hphMX6 Δrpl41A::natMX6 Δrpl41B::natMX6*	This study
TYSC572	eB12Δ eL41Δ	*MAT**a** ura3-52 leu2Δ1 his3Δ200 trp1Δ36 Δarg4 Δlys1 Δrpl19A::kanMX6 Δrpl19B::kanMX6 Δrpl41A::natMX6 Δrpl41B::natMX6 [pRS315-rpl19$_{1-146}$]*	This study
TYSC603	AL-Δ2	*MAT**a** ura3-52 leu2Δ1 his3Δ200 trp1Δ36 Δarg4 Δlys1 Δrpl19A::kanMX6 Δrpl19B::kanMX6 Δrpl24A::hphMX6 Δrpl24B::hphMX6 [pRS315-rpl19$_{1-146}$; pRS314-rpl24$_{1-65}$]*	This study
TYSC624	AL-Δ3	*MAT**a** ura3-52 leu2Δ1 his3Δ200 trp1Δ36 Δarg4 Δlys1 Δrpl19A::kanMX6 Δrpl19B::kanMX6 Δrpl24A::hphMX6 Δrpl24B::hphMX6 Δrpl41A::natMX6 Δrpl41B::natMX6 [pRS315-rpl19$_{1-146}$; pRS314-rpl24$_{1-65}$]*	This study

Materials and Methods

Visualization of ribosome and r-protein structures

PyMOL 1.5.0.5 (Schrodinger 2015) was used to visualize and compare the structures of eukaryotic (*Saccharomyces cerevisiae*) and archaeal (*Haloarcula marismortui*) ribosomes and r-proteins. Coordinates for yeast (PDB entry 3U5E form (Ben-Shem et al. 2011)) and archaeal (PDB entry 4V9F from (Gabdulkhakov et al. 2013)) ribosomes were used.

Preparation of 80S ribosomes for mass spectrometric analysis

To label proteins in yeast cells with 'light' amino acids, wild-type, AL-2Δ and AL-3Δ (TYSC309, TYSC603 and TYSC624) cells were grown in YPD medium. To label proteins with 'heavy' amino acids, wild-type cells were grown as described previously (Kisly et al. 2019). The 'light' and 'heavy' labelled ribosomes were purified as described previously (Kisly et al. 2019), except high-magnesium buffer A30 (30 mM Hepes-KOH [pH 7.5], 30 mM $Mg(OAc)_2$, 100 mM KCl, 2 mM DTT) + 0.5 mM PMSF (final conc.) was used for ribosome purification. Additionally, 80S fractions were not pelleted by ultracentrifugation, but concentrated with 100,000 NMWL Amicon Ultra-15 filters in buffer A30. 'Light' and 'heavy' ribosomes were mixed and precipitated as described previously (Kisly et al. 2019). Proteins were reduced for 1 hour at RT by adding 5 mM DTT and carbamidomethylated with 20 mM chloroacetamide for 1 hour at RT in the dark. Proteins were digested with endoproteinase Lys-C (Wako) at an enzyme to protein ratio 1:50 for 4 hours at RT. The urea concentration in the solutions was reduced by adding 4 volumes of 100 mM NH_3HCO_3 and peptides were further digested with mass spectrometry grade trypsin (Sigma Aldrich; enzyme to protein ratio 1:50) at RT for overnight. Enzymes were inactivated by addition of TFA to a final concentration of 1%.

LC-MS/MS analysis

Two independent biological replicates for each strain were analyzed. Peptides were desalted on self-made reverse-phase C_{18} stop and go extraction tips. Samples were injected to an Ultimate 3000 RSLCnano system (Dionex) using a C18 trap-column (Dionex) and an in-house packed (3 µm C18 particles, Dr Maisch) analytical 50 cm x 75 µm emitter-column (New Objective). Peptides were eluted at 200 nl/min with a 5-40% B 120 min gradient (buffer B: 80% acetonitrile + 0.1% formic acid, buffer A: 0.1% formic acid) to a Q Exactive Plus (Thermo Fisher Scientific) mass spectrometer (MS) using a nano-electrospray source (spray voltage of 2.5 kV). The MS was operated with a top-10 data-dependent acquisition strategy. Briefly, one 350-1400 m/z MS scan at a resolution setting of R=70 000 at 200 m/z was followed by higher-energy collisional dissociation fragmentation (normalized collision energy of 26) of 10 most intense ions (z: +2 to +6) at R=17 500. MS and MS/MS ion target values were 3e6 and 5e4 with 50 ms injection times. Dynamic exclusion was limited to 40 s.

Raw mass spectrometric data files were processed using MaxQuant software and searched against Saccharomyces Genome Database proteins sequences of all systematically named ORFs as described previously (Piir et al. 2014; Kisly et al. 2019). Obtained data file containing all detected peptides was further processed in RStudio, and 'heavy'/'light' ratios were calculated as described previously (Kisly et al. 2019). To compare ratios of eL19 and eL24 proteins more precisely, the identical peptides originated from eL19 and eL24 were analyzed in wild-type and mutant strains. Statistical significance of changes in protein ratios was evaluated in Perseus by the unpaired two-sample Student's t-test. For ribosomal proteins, fold change higher or lower than 1.41 times ($\log_2 >= 0.5$ or $\log_2 <= -0.5$) and *P*-value lower than 0.05 ($-\log_{10} > 1.3$) were defined as statistically significant thresholds of difference.

References

Ben-Shem A, Garreau de Loubresse N, Melnikov S, Jenner L, Yusupova G, Yusupov M. 2011. The structure of the eukaryotic ribosome at 3.0 A resolution. *Science* **334**: 1524-1529.

Gabdulkhakov A, Nikonov S, Garber M. 2013. Revisiting the Haloarcula marismortui 50S ribosomal subunit model. *Acta crystallographica Section D, Biological crystallography* **69**: 997-1004.

Kisly I, Gulay SP, Maeorg U, Dinman JD, Remme J, Tamm T. 2016. The Functional Role of eL19 and eB12 Intersubunit Bridge in the Eukaryotic Ribosome. *Journal of molecular biology* **428**: 2203-2216.

Kisly I, Remme J, Tamm T. 2019. Ribosomal protein eL24, involved in two intersubunit bridges, stimulates translation initiation and elongation. *Nucleic acids research* **47**: 406-420.

Piir K, Tamm T, Kisly I, Tammsalu T, Remme J. 2014. Stepwise splitting of ribosomal proteins from yeast ribosomes by LiCl. *PloS one* **9**: e101561.

Schrodinger, LLC. 2015. The PyMOL Molecular Graphics System, Version 1.5.0.5.

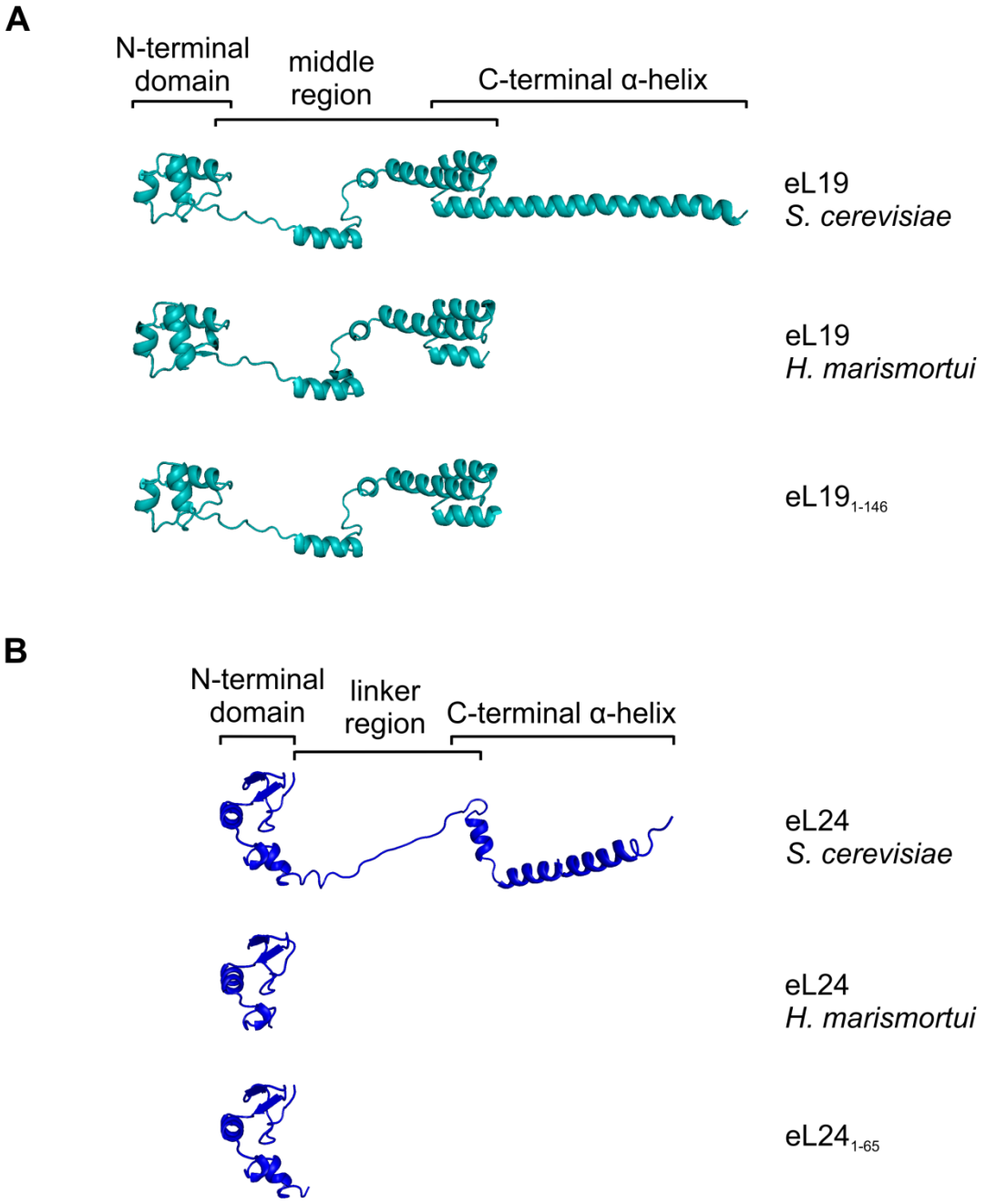

Figure S1. Structures of the r-proteins eL19 (A) and eL24 (B).

Structures of the wild-type eukaryotic (*Saccharomyces cerevisiae*) and archaeal (*Haloarcula marismortui*) r-proteins eL19 and eL24 are shown. Variants of budding yeast $eL19_{1\text{-}146}$ and $eL24_{1\text{-}65}$ mimicking the archaeal versions are also presented. The domain organization of both r-proteins is indicated.

Figure S2 (A, B)

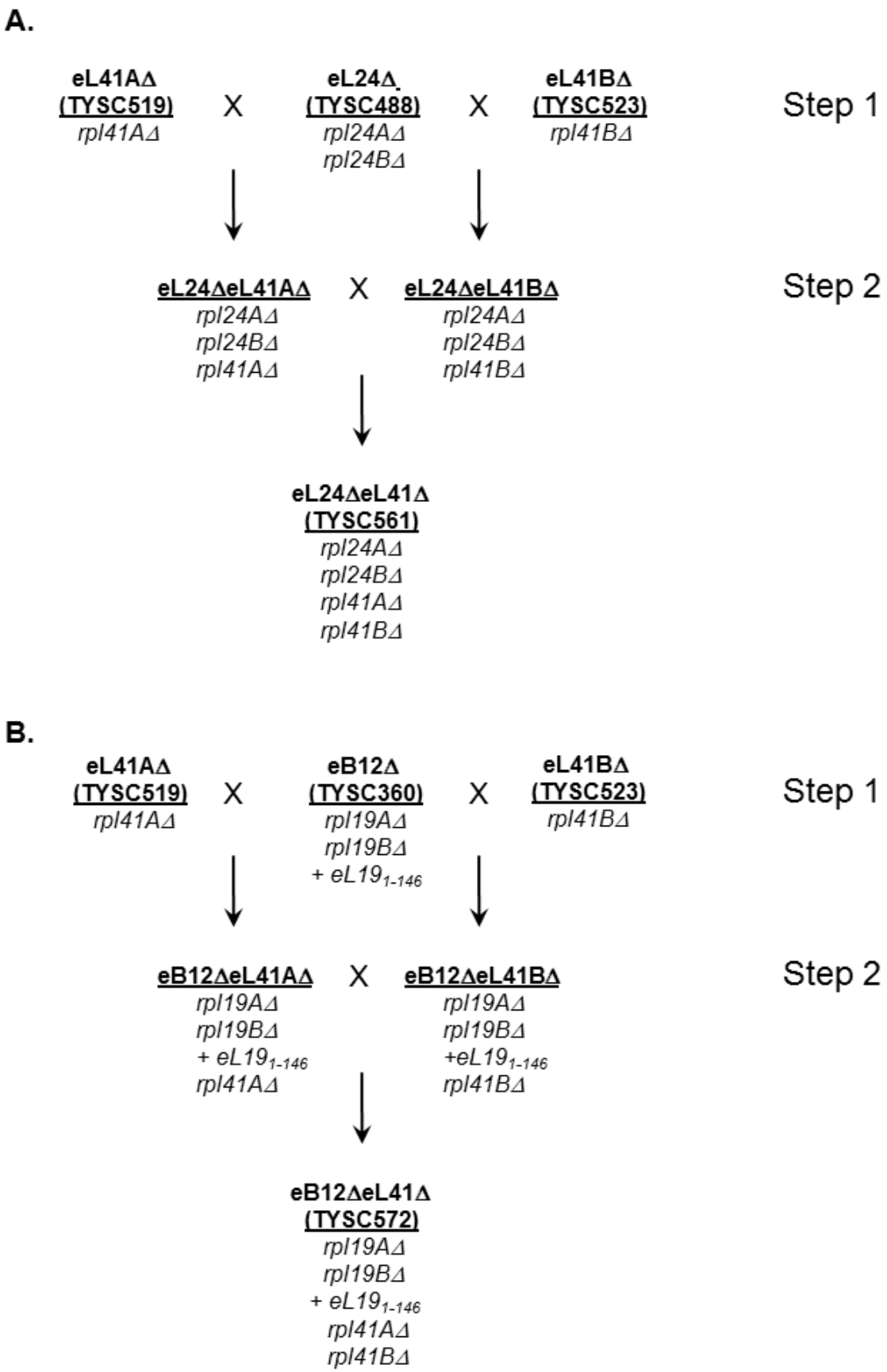
A.
eL41AΔ
(TYSC519)
rpl41AΔ
X
eL24Δ
(TYSC488)
rpl24AΔ
rpl24BΔ
X
eL41BΔ
(TYSC523)
rpl41BΔ
Step 1
eL24ΔeL41AΔ
rpl24AΔ
rpl24BΔ
rpl41AΔ
X
eL24ΔeL41BΔ
rpl24AΔ
rpl24BΔ
rpl41BΔ
Step 2
eL24ΔeL41Δ
(TYSC561)
rpl24AΔ
rpl24BΔ
rpl41AΔ
rpl41BΔ
B.
eL41AΔ
(TYSC519)
rpl41AΔ
X
eB12Δ
(TYSC360)
rpl19AΔ
rpl19BΔ
+ eL19 1-146
X
eL41BΔ
(TYSC523)
rpl41BΔ
Step 1
eB12ΔeL41AΔ
rpl19AΔ
rpl19BΔ
+ eL19 1-146
rpl41AΔ
X
eB12ΔeL41BΔ
rpl19AΔ
rpl19BΔ
+eL19 1-146
rpl41BΔ
Step 2
eB12ΔeL41Δ
(TYSC572)
rpl19AΔ
rpl19BΔ
+ eL19 1-146
rpl41AΔ
rpl41BΔ

Figure S2 (C, D)

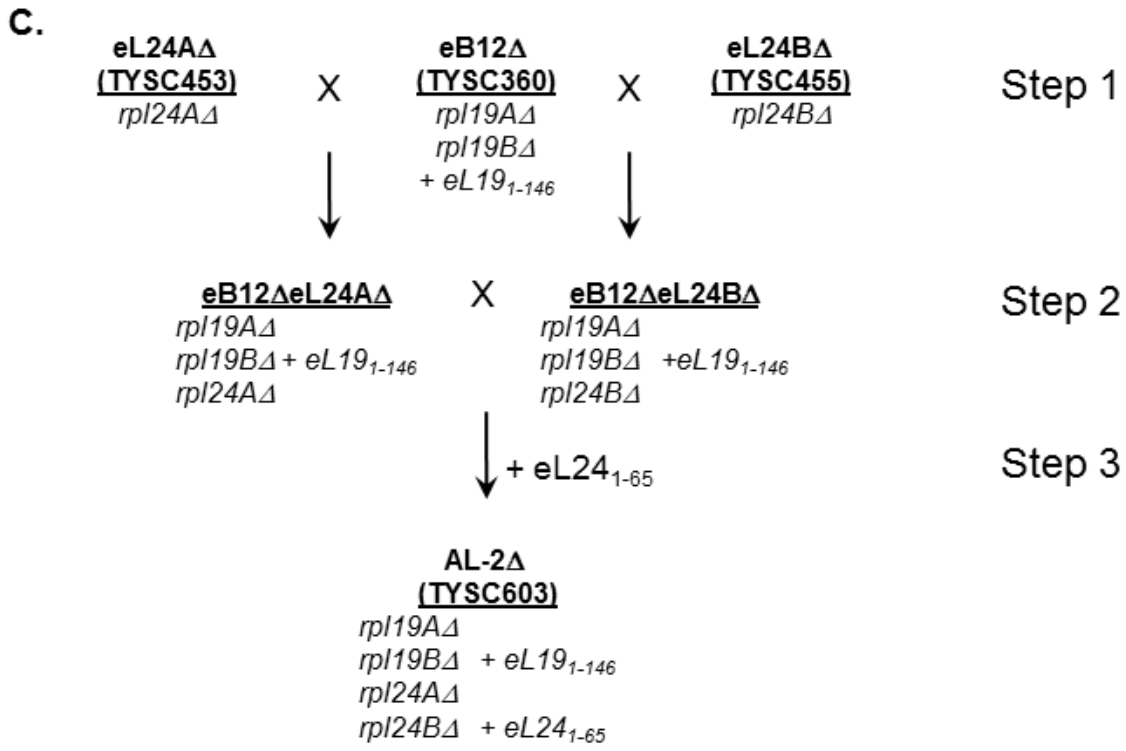
C.
eL24AΔ
(TYSC453)
rpl24AΔ
X
eB12Δ
(TYSC360)
rpl19AΔ
rpl19BΔ
+ eL19 1-146
X
eL24BΔ
(TYSC455)
rpl24BΔ
Step 1
eB12ΔeL24AΔ
rpl19AΔ
rpl19BΔ + eL19 1-146
rpl24AΔ
X
eB12ΔeL24BΔ
rpl19AΔ
rpl19BΔ +eL19 1-146
rpl24BΔ
Step 2
+ eL24 1-65
Step 3
AL-2Δ
(TYSC603)
rpl19AΔ
rpl19BΔ + eL19 1-146
rpl24AΔ
rpl24BΔ + eL24 1-65

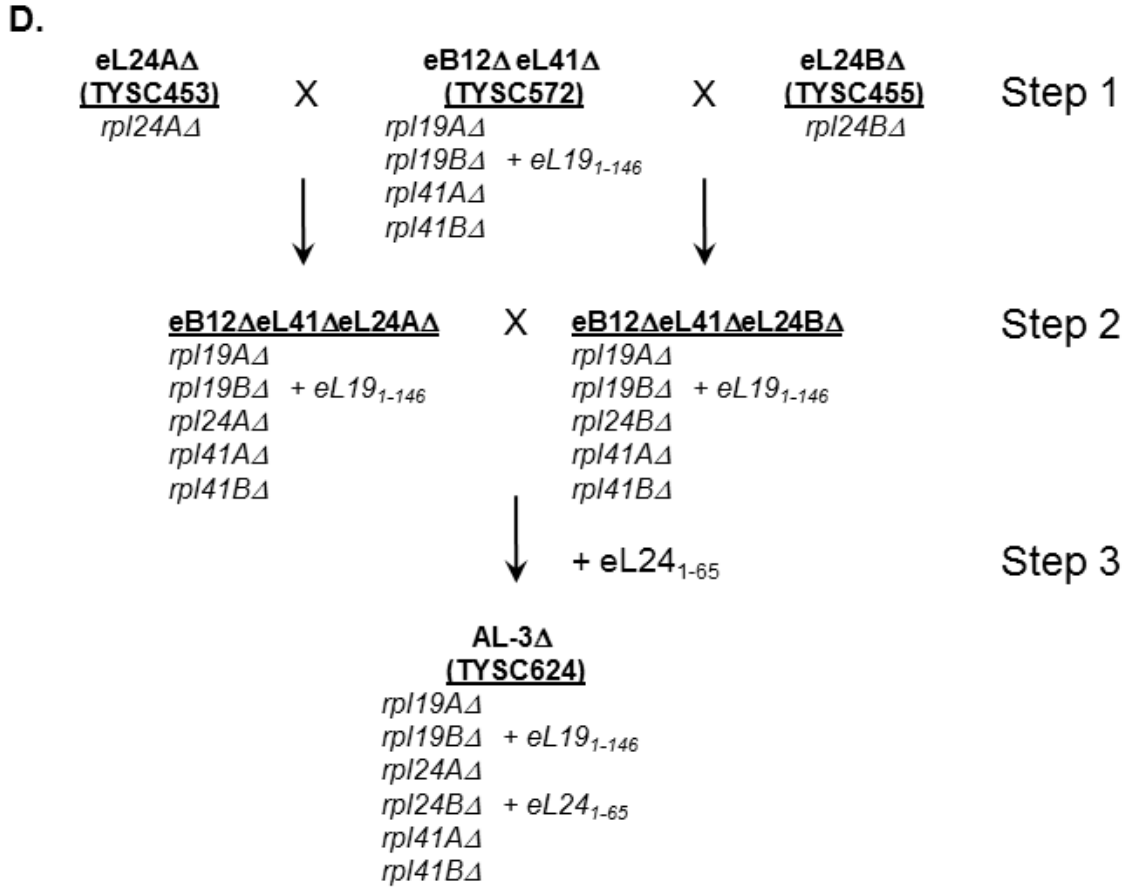
D.
eL24AΔ
(TYSC453)
rpl24AΔ
X
eB12Δ eL41Δ
(TYSC572)
rpl19AΔ
rpl19BΔ + eL19 1-146
rpl41AΔ
rpl41BΔ
X
eL24BΔ
(TYSC455)
rpl24BΔ
Step 1
eB12ΔeL41ΔeL24AΔ
rpl19AΔ
rpl19BΔ + eL19 1-146
rpl24AΔ
rpl41AΔ
rpl41BΔ
X
eB12ΔeL41ΔeL24BΔ
rpl19AΔ
rpl19BΔ + eL19 1-146
rpl24BΔ
rpl41AΔ
rpl41BΔ
Step 2
+ eL24 1-65
Step 3
AL-3Δ
(TYSC624)
rpl19AΔ
rpl19BΔ + eL19 1-146
rpl24AΔ
rpl24BΔ + eL24 1-65
rpl41AΔ
rpl41BΔ

Figure S2. Diagrams illustrating the strategy for strain construction.

(A) Strategy for construction of eL24ΔeL41Δ strain (TYSC561).

Step 1: Strain *rpl24AΔrpl24BΔ* (eL24Δ, TYSC488) was crossed with mutants carrying either *rpl41AΔ* or *rpl41BΔ*. Strains *eL24Δrpl41AΔ* and *eL24Δrpl41BΔ* were isolated.

Step 2: Strains obtained from the first cross were mated and strain carrying the deletion of eL24 and eL41 encoding paralogous genes (eL24ΔeL41Δ) was isolated.

(B) Strategy for construction of eB12ΔeL41Δ strain (TYSC572).

Step 1: Strain *rpl19AΔrpl19BΔ* + $eL19_{1\text{-}146}$ (eB12Δ, TYSC360) was crossed with mutants carrying either *rpl41AΔ* or *rpl41BΔ*. Strains *eB12Δrpl41AΔ* and *eB12Δrpl41BΔ* were isolated.

Step 2: Strains obtained from the first cross were mated and a strain with a plasmid for expression of archaeal variant of eL19 ($eL19_{1\text{-}146}$) and carrying the deletions of eL19 and eL41 encoding paralogous genes (eB12ΔeL41Δ) was isolated.

(C) Strategy for construction of AL-Δ2 strain (TYSC603).

Step 1: Strain *rpl19AΔrpl19BΔ* + $eL19_{1\text{-}146}$ (eB12Δ, TYSC360) was crossed with mutants carrying either *rpl24AΔ* or *rpl24BΔ*. Strains *eB12Δrpl24AΔ* and *eB12Δrpl24BΔ* were isolated.

Step 2: Strains obtained from the first cross were mated.

Step 3: The plasmid expressing an archaeal variant of eL24 ($eL24_{1\text{-}65}$) was transformed into the heterozygous diploid before sporulation was induced. The strain carrying deletion of eL19 and eL24 encoding paralogous genes and containing the plasmids for expression of $eL19_{1\text{-}146}$ and $eL24_{1\text{-}65}$ (AL-Δ2) was isolated.

(D) Strategy for construction of AL-Δ3 strain (TYSC624).

Step 1: Strain *rpl19AΔrpl19BΔ rpl41AΔ rpl41BΔ* + $eL19_{1\text{-}146}$ (eB12ΔeL41Δ, TYSC572) was crossed with mutants carrying either *rpl24AΔ* or *rpl24BΔ*. Strains *eB12ΔeL41Δrpl24AΔ* and *eB12ΔeL41Δrpl24BΔ* were isolated.

Step 2: Strains obtained from the first cross were mated.

Step3: The plasmid expressing an archaeal variant of eL24 ($eL24_{1-65}$) was transformed into the heterozygous diploid before sporulation was induced. The strain carrying deletions of eL19, eL24 and eL41 encoding paralogous genes and containing the plasmids for expression of $eL19_{1-146}$ and $eL24_{1-65}$ (AL-Δ3) was isolated.

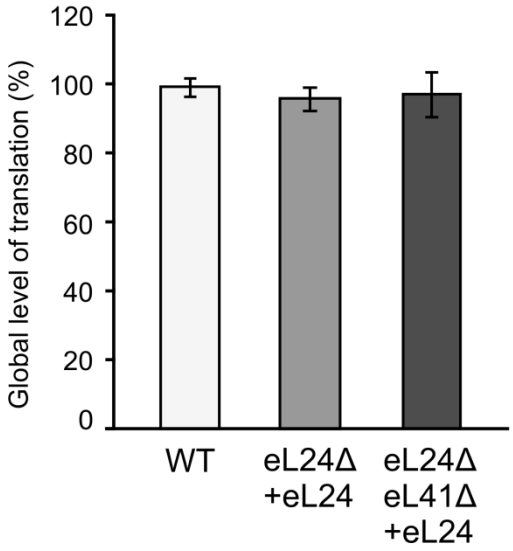

Figure S3. Analysis of global levels of translation of eL24 mutants.

Wild-type (WT, TYSC309), *rpl24AΔrpl24BΔ* strain (eL24Δ, TYSC488) expressing the wild-type allele of eL24, and *rpl24AΔrpl24BΔ* strain carrying the deletions of eL41 encoding genes (eL24ΔeL41Δ, TYSC561) and expressing the wild-type allele of eL24 were analyzed. The incorporation of radioactive isotope-labeled amino acids into newly synthesized polypeptides was measured in exponentially growing cells at 30°C. Samples were taken every 15 minutes for 2 hours. The samples were TCA precipitated, and the incorporation of radioactive label over time was measured. The obtained values of disintegrations per minute (DPM) were plotted, and the slope was calculated. The average slope values (mean ± SD) from at least four biological replicates are plotted. No statistically significant difference was determined by the Games-Howell *post hoc* test at the significance level of 0.05.

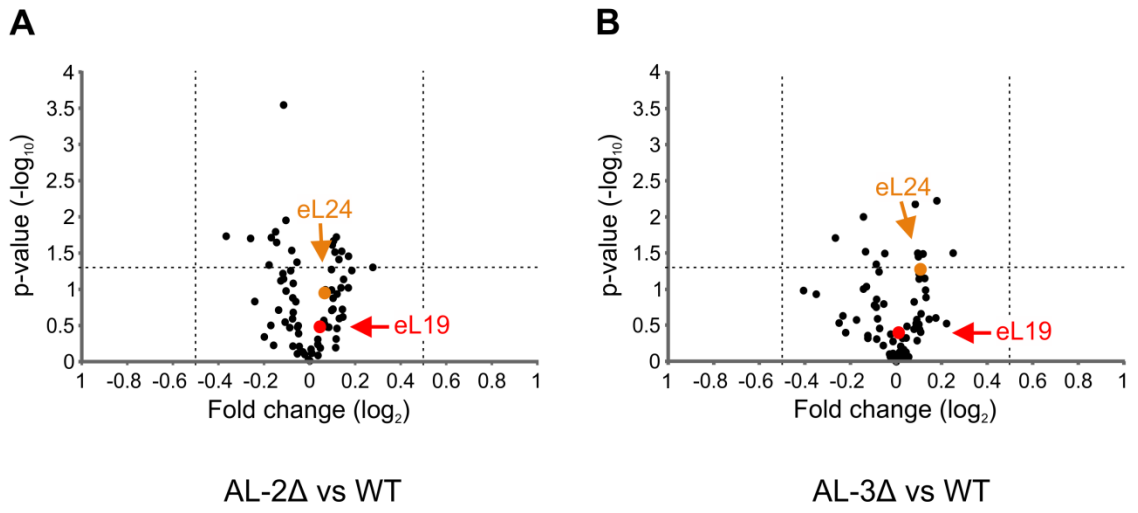

Figure S4. Mass spectrometric analysis of ribosomes from Archaea-like mutants.

Volcano plots of changes in r-protein composition in ribosomes of AL-2Δ mutant vs ribosomes from wild type (A) and ribosomes of AL-3Δ mutant vs ribosomes from wild type (B). Vertical dashed lines highlight the fold change cutoff of 1.41 (log_2 = 0.5 and -0.5). Horizontal dashed line highlights the significance cutoff of 0.05 ($-log_{10}$ = 1.3). Red and orange circles indicate the r-proteins eL19 and eL24, respectively.

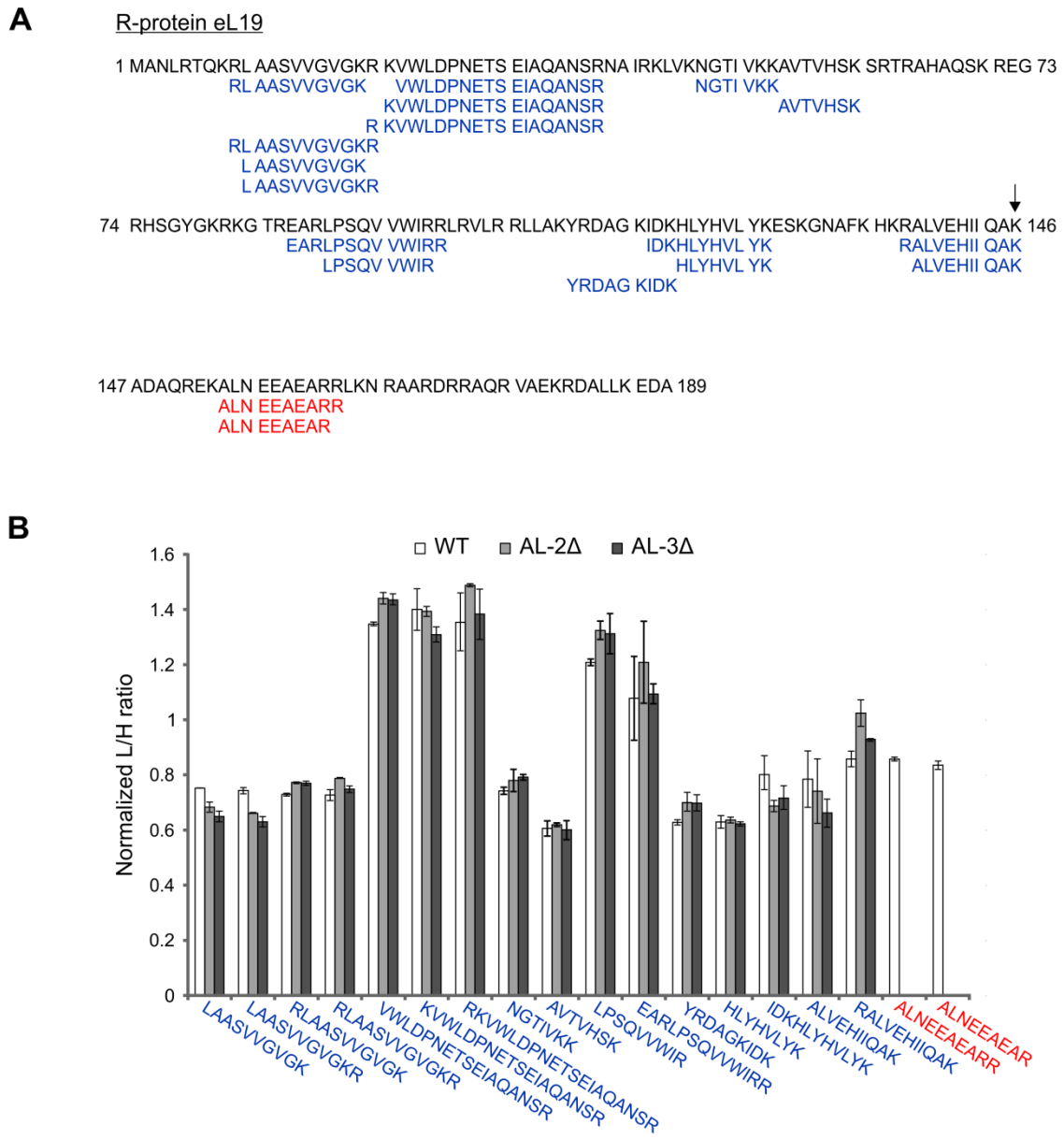

Figure S5. Position (A) and "light/heavy" ratios (B) of peptides originated from the r-protein eL19.

Sequence of the eL19 is presented in black letters. Arrow indicates position of the last amino acid residue in archaeal variant of eL19 in ribosomes of AL-2Δ and AL-3Δ mutants. Peptides identified in ribosomes of all strains and biological replicates are shown in blue letters. Peptides identified only in ribosomes of wild-type strain are shown in red letters. The average "light/heavy" ratios (mean ± SD) across all biological replicates are plotted.

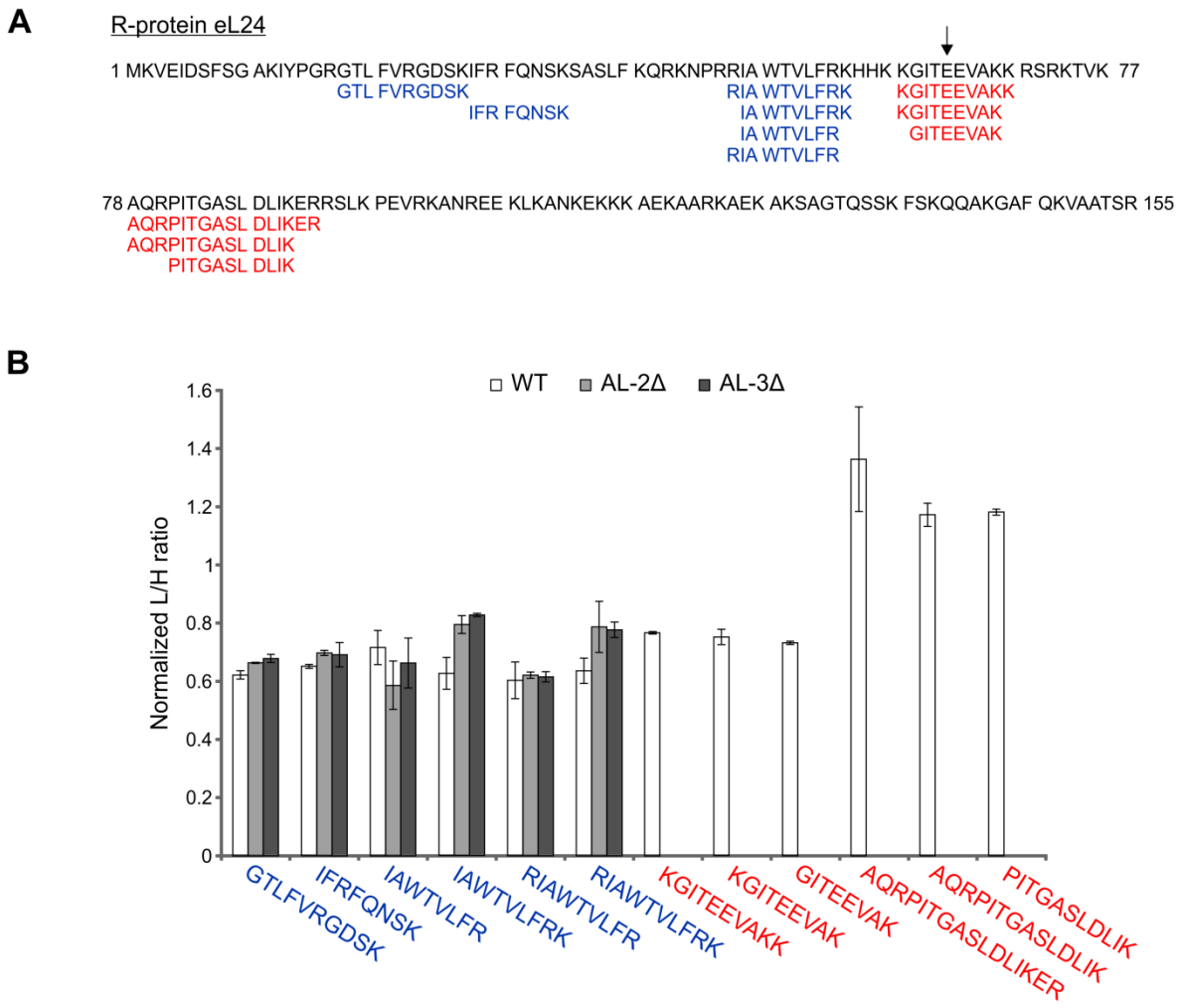

Figure S6. Position (A) and "light/heavy" ratios (B) of peptides originated from the r-protein eL24.

Sequence of the eL24 is presented in black letters. Arrow indicates position of the last amino acid residue in archaeal variant of eL24 in ribosomes of AL-2Δ and AL-3Δ mutants. Peptides identified in ribosomes of all strains and biological replicates are shown in blue letters. Peptides identified only in ribosomes of wild-type strain are shown in red letters. The average "light/heavy" ratios (mean ± SD) across all biological replicates are plotted.